Materials and Design 97 (2016) 424–430

Contents lists available at ScienceDirect

Materials and Design

journal homepage: www.elsevier.com/locate/matdes

Fabrication of CNT/Al composites with low damage to CNTs by a novel solution-assisted wet mixing combined with powder metallurgy processing

Z.Y. Liu [a], K. Zhao [a], B.L. Xiao [a], W.G. Wang [b], Z.Y. Ma [a,*]

[a] Shenyang National Laboratory for Materials Science, Institute of Metal Research, Chinese Academy of Sciences, 72 Wenhua Road, Shenyang 110016, China
[b] Liaoning Shihua University, 1 Dandong Road, Fushun 113001, China

ARTICLE INFO

Article history:
Received 19 December 2015
Received in revised form 25 February 2016
Accepted 27 February 2016
Available online 03 March 2016

Keywords:
Metal-matrix composites
Carbon nanotube
Wet mixing
Powder metallurgy
Mechanical properties
Microstructures

ABSTRACT

A novel solution-assisted wet mixing processing was developed to efficiently produce CNT/Al composite powders. CNTs were firstly dispersed in zwitterionic surfactant aqueous solution, and then the flaky Al powders, produced from spherical Al powders by ball milling, were mixed with the CNT solution to adsorb the dispersed CNTs in the solution. It was indicated that CNTs could be uniformly adsorbed onto the flaky Al powders and CNT/Al powders with a maximum CNT concentration of 7.5 vol% could be obtained after filtering and drying. 1.5 and 3 vol% CNT/Al composites were then fabricated using the resultant composite powders through a powder metallurgy route. CNTs with average lengths of 0.9 μm and well-retained wall structure were uniformly dispersed in the Al matrix and aligned arrangement of CNTs was achieved after hot forging. Furthermore, it was found that most of CNTs were distributed at the grain boundaries and the CNT-Al interfaces were well bonded. The strengths of the CNT/Al composites were significantly increased, which could be attributed to the efficient load transfer of CNTs.

1. Introduction

With high specific strength and modulus, aluminum matrix composites are effective to improve fuel efficiency by weight reduction in transportation and aircraft industries [1–3]. Carbon nanotubes (CNTs) are considered as an ideal reinforcement for aluminum matrix composites due to their extremely high strength (~30 GPa) and modulus (~1 TPa) as well as low density and good physical properties [4–7]. However, to disperse CNTs into metal matrices is a difficult task, because of entanglement or bundling of the CNT clusters resulting from strong van der waals force and large aspect ratio [8–9].

In the past few years, many dispersion methods, for example mechanical dispersion [10–16], molecular level mixing [17–18], in-situ CNT growth on metal powders [19–20], have been tried to disperse CNTs into the metal matrices. Among the reported methods, the mechanical dispersion processes (like ball milling, friction stir processing) encounter the problem of CNT structural damage. The molecular level mixing is only suitable for fabricating CNTs reinforced Cu, Co and Ni matrix composites. In-situ CNT growth had the impurity problems of catalyst particles and was hardly compatible with industrial production routes.

Many other investigators turned solution-assisted wet mixing process to disperse CNTs with little structure damage. Cho et al. [21] mixed functionalized CNT ethanol solution with spherical Cu powders under ultrasonic and obtained well dispersed CNT/Cu powders. However, Deng et al. [22] indicated that CNT clusters still existed when they mixed functionalized CNT ethanol solution with Al powders using a similar method. Liao et al. [23] found that CNTs could be dispersed by an anionic surfactant assisted mixing method; however CNTs were distributed along the Al grain boundaries as clusters. Kondoh et al. [24–26] used a zwitterionic surfactant aqueous solution to help dispersing CNTs and mixing CNTs-metal powders. CNT/Al, CNT/Mg or CNT/Ti powders were then obtained by drying the mixtures. However, CNT clusters could not be completely avoided as a result of CNT aggregation during drying as well as small specific surface area of spherical metal powders.

Jiang et al. [27] found that the Al powders functionalized with –OH could adsorb CNTs functionalized with –COOH. Uniformly dispersed CNT/Al powders were successfully fabricated by mixing the functionalized Al powders with CNT-sodium dodecyl benzene sulfonate (SDBS) aqueous solution. They also found that flaky Al powders with large specific surface areas could provide more sites to adsorb high concentration of CNTs. However, functionalization treatment of Al powders and rinsing the SDBS were time-consuming, and thus greatly reduced the efficiency and increased the risk of reaction between Al powders and water.

Clearly, an efficient solution-assisted wet mixing method is still highly desirable. Such a method should meet the following requirements. Firstly, CNTs should be well dispersed in a solvent and the solvent/dispersants are easily decomposed prior to composite compaction. Secondly, flaky aluminum powders should be obtained to provide enough surfaces for CNT locating. Ball milling is usually used

* Corresponding author.
E-mail address: zyma@imr.ac.cn (Z.Y. Ma).

http://dx.doi.org/10.1016/j.matdes.2016.02.121
0264-1275/

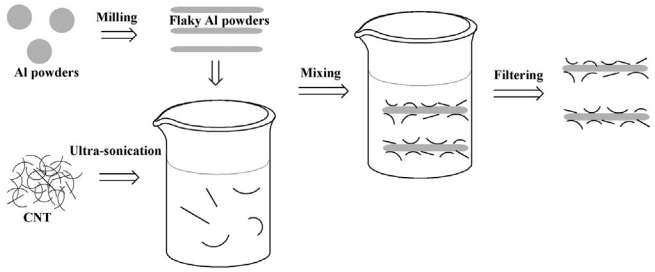

Fig. 1. Fabrication schematic of CNT/Al composite powders.

to produce flaky Al powders with different thicknesses. Thirdly, CNTs can be easily dispersed onto aluminum powders and no clusters are formed during drying. Furthermore, no pre-treatment should be adopted to aluminum powders.

In this study, a simple strategy for a solution-assisted wet mixing method was developed to solve the problems of CNT distribution on Al powders. 1.5 and 3 vol% CNT/Al composites were then fabricated using a conventional powder metallurgy process, including cold compacting, hot pressing and hot forging. The aim of this study is to establish an efficient route of dispersing CNTs into Al matrix and investigate the load-transfer efficiency of CNTs in the Al matrix.

2. Experimental

2.1. Raw materials

As-received clustered multi-walled CNTs, with a diameter of 10–40 nm and a length of 0.5–2 μm, fabricated by chemical vapor deposition and then functionalized with carboxyl (−COOH), were provided by Chengdu Organic Chemistry Co. Ltd., China. The as-received spherical Al powders had an average diameter of ~10 μm. 3-(*N*,*N*-dimethylmyristylammonio) propanesulfonate, a typical zwitterionic surfactant was supplied by Aladdin-Holdings Group Co. Ltd, China.

2.2. Preparation of CNT/Al powders

Fig. 1 illustrates the fabrication flow of CNT/Al composite powders. In a typical flow of solution-assisted wet mixing process, three steps were needed.

2.2.1. Preparation of CNT aqueous solution

0.5 wt% zwitterionic surfactant, which was used to disperse a high weight fraction of CNTs in water, and 5 mg/ml CNTs were introduced into deionized water and sonicated for 2 h to get an ink-like suspension.

2.2.2. Preparation of flaky Al powders

500 g spherical Al powders was placed in stainless steel mixing jars containing 7.5 kg stainless steel balls of 5 mm diameter. 1.5 wt% stearic acid and 2 L ethanol were added into the jars to avoid cold-welding of the Al powders. The ball milling was conducted at a rotation rate of 350 rpm for 3 h with water cooling to obtain flaky Al powders slurry. Then the slurry was filtered and dried to obtain flaky Al powders.

Table 1
I_G/I_D of the CNT in suspensions at different sonication time.

Sonication time (h)	0	1	2
I_G/I_D	1.39	1.37	1.32

2.2.3. Adsorption of CNTs on flaky Al powders

The CNT aqueous dispersion was stirred and the flaky Al powders were added slowly. The mixed slurry was stirred until its color changed from black to transparent, then filtered to obtain the CNT/Al composite powders. Finally, the powders were vacuum dried (10^0 ~ 10^1 Pa) at 333 K for 5 h. Three concentrations (1.5, 3, 7.5 vol%) of CNT/Al powders were obtained.

2.3. Consolidation of CNT/Al composites

The dried (1.5, 3 and 7.5 vol%) CNT/Al powders were cold-compacted in a cylinder die, degassed (773 K for 1 h) and hot-pressed (853 K for 1 h) into cylindrical billets with a diameter of 55 mm and a height of 50 mm. The as-pressed billets were hot forged with steel canning at 753 K into disk plates with a thickness of about 10 mm and a diameter of about 150 mm. For comparison, the pure Al sample was also fabricated using the same route.

2.4. Characterization of CNT/Al composites

The flaky Al powders were observed using the optical microscopy (OM, Zeiss Axiovert 200 MAT) and field emission scanning electron microscopy (FESEM, Leo Supra 55). Thickness of flaky Al powders were obtained by measuring at least 50 flaky Al powders in the OM photos. The sonicated CNT-zwitterionic aqueous solution was dropped on a Cu net coated with carbon member. The Cu net was washed by dropping acetone and then dried for transmission electron microscopy (TEM, Tecnai G2 20) observation to estimate CNT distribution and length in aqueous solution. CNT distributions on the flaky Al powders and Al matrix were examined using FESEM and TEM, respectively. The CNT-Al interface and CNT structure were observed by high resolution TEM (HRTEM, Tecnai G2 20). The specimens for TEM were machined in the radial direction from the forged disk-samples.

Raman spectroscopic measurements were conducted using the JY Labram HR800 (excitation about 1 μm). The peak intensity ratio of G-line (graphite) and D-line (defect), namely I_G/I_D was calculated to provide information about the quality of CNTs. Tensile tests with a gauge length of 5 mm, a width of 1.5 mm and a thickness of 1 mm were machined in the radial direction from the forged disk-samples. The tensile specimens were conducted at a strain rate of $1 \times 10^{-3}\ s^{-1}$ at room temperature on an Instron 5848 tester.

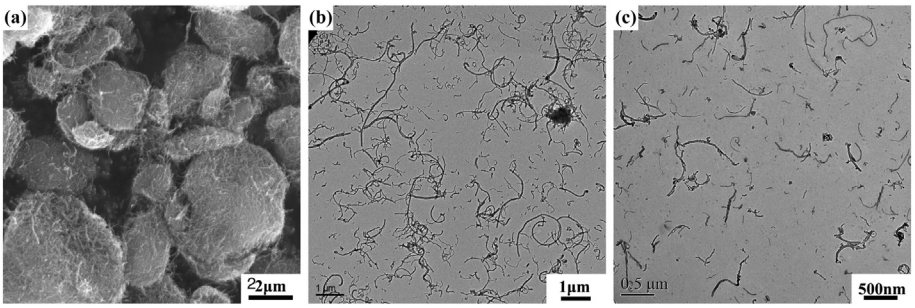

Fig. 2. (a) As-received CNT and CNT distribution in solution with ultrasonic durations of (b) 1 h and (c) 2 h.

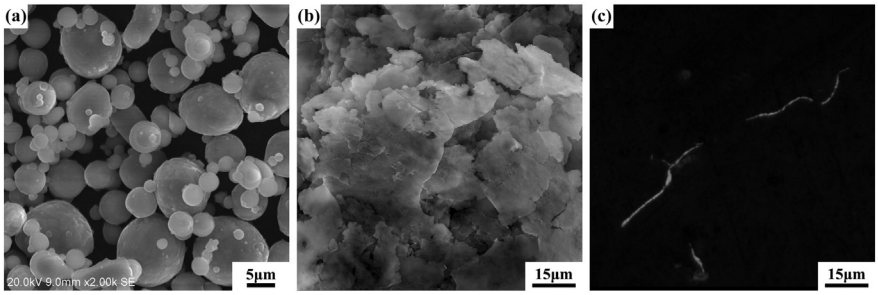

Fig. 3. SEM morphology of (a) as-received Al powders, (b) flaky Al powders and (c) OM morphology of flaky Al powders.

3. Results and discussion

3.1. Characterization of CNT aqueous solution and flaky Al powders

Fig. 2 shows the as-received CNTs and CNT distribution in zwitterionic surfactant aqueous solution at different ultrasonic treatment durations. The as-received CNTs were clusters with sizes of about 2 μm (Fig. 2(a)). CNT clusters were greatly reduced after 1 h ultrasonic treatment, though small clusters could still be observed (Fig. 2(b)). After 2 h, nearly no CNT clusters could be found. The disassembling of CNTs could be attributed to dipole/dipole electrostatic interactions and hydrophilic/hydrophilic interaction of the zwitterionic surfactant, which was reported by Fugetsu et al. [28]. It is noted that CNT length decreased after ultrasonication, attributable to increased energy input [29].

Raman spectrum results in Table 1 shows a slightly decreased I_G/I_D value with increasing ultrasonic duration, indicating that CNT damage slightly increased as ultrasonic duration increased. 2 h ultrasonic duration was determined to be optimized time to uniformly disperse CNTs and reduce the structure damage of CNTs.

Fig. 3 shows the as-received Al powder and flaky Al powder morphology after 3 h milling. As-received spherical Al powders (Fig. 3(a)) changed to flaky morphology after 3 h milling (Fig. 3(b)), due to the intense shear effect during milling. The thickness of the flaky Al powders was about 0.5 μm, which indicating greatly increased specific surface area of flaky Al powders compared with that of the as-received spherical Al powders. Fe and aluminum oxide are two common contaminations which were easily introduced during milling. Because the CNT/Al composites were fabricated using the same flaky Al powders as the matrix, the contaminations led to same effects to the composites with different CNT concentrations. As a result, the contaminations were not discussed in the following text.

3.2. CNT adsorption mechanism and CNT distribution on Al powders

Fig. 4(a) shows the mixture of the CNT-SDBS aqueous solution/Al powders and CNT-zwitterionic surfactant aqueous solution/Al powders after mechanical stirring. For the CNT-SDBS aqueous solution and Al mixture, the upper layer of the mixture remains black, suggesting that most of CNTs were still in suspension and were not adsorbed onto the Al surfaces. In contrast, the upper layer of the CNT-zwitterionic surfactant aqueous solution and Al powders mixture is transparent, indicated that most of CNTs in the suspension have been adsorbed onto the Al surfaces. SDBS also has the ability to disperse high weight fraction of CNTs in water by the hydrophilic/hydrophilic interaction [30]. However, CNTs dispersed in SDBS aqueous solution could not be adsorbed onto flaky Al powders. This implies that the special dipole/dipole electrostatic interactions of the zwitterionic surfactant could be the reason that CNTs could be adsorbed onto Al powders.

According to the knowledge of the zwitterionic surfactant self-assembly, the zwitterionic surfactants with a positive charge and a negative charge on their headgroups of each molecule form diads and/or quartets because of the electrostatic interactions. As shown in Fig. 4

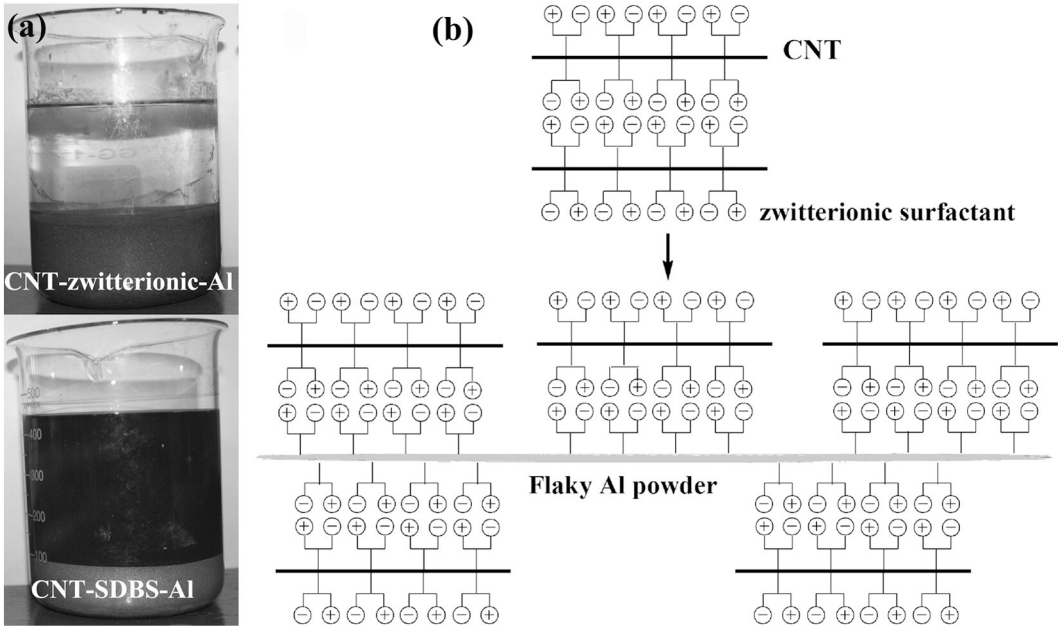

Fig. 4. (a) CNT-Al suspension after adsorption and (b) schematic of CNT adsorption on flaky Al powders.

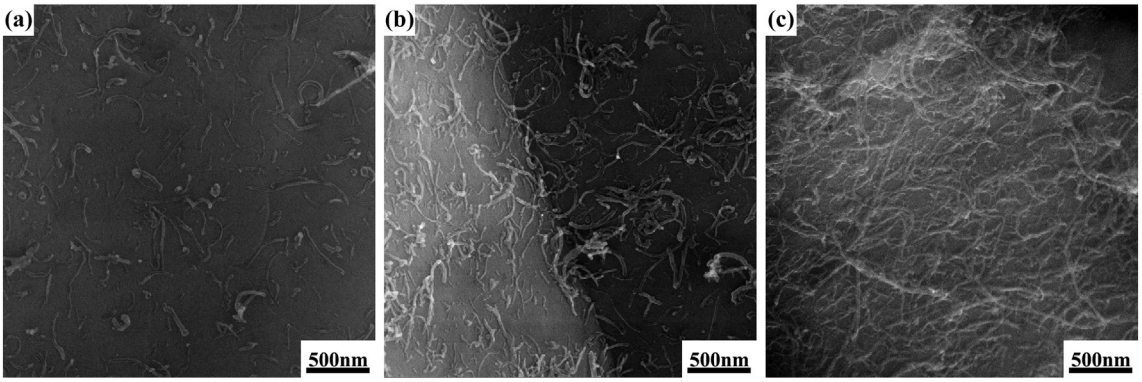

Fig. 5. CNT distribution of CNT/Al powders with different concentrations: (a) 1.5 vol%, (b) 3 vol%, (c) 7.5 vol%.

(b), when mixed with CNTs or Al powders, zwitterionic surfactant forms the self-assembled diads and/or quartets as a result of the electrostatic attraction. The sulfonate/quaternary-ammonium headgroups orientate toward the terminal-end, and most of them form anti-parallel doublets. The self-assembled zwitterionic surfactant monolayer should have high propensities to interact with the others because of the strong dipole/dipole electrostatic interactions. The adsorption of CNTs on Al powders is attributed to the strong dipole/dipole electrostatic interactions between zwitterionic monolayers on CNTs and Al powders.

Fig. 5 shows the CNT distribution on the Al powders prepared by the solution-assisted wet mixing process (the composite powders were heat treated at 773 K for 1 h). CNTs were uniformly adsorbed on the flaky Al powders, and nearly no CNT clusters could be observed. For 1.5 vol% CNT/Al composite powders, CNTs were sparsely adsorbed on the flaky Al powders (Fig. 5(a)). About 50% of the surfaces of flaky Al powders were covered by CNTs for 3 vol% CNT/Al composite powders (Fig. 5(b)). For 7.5 vol% CNTs/Al composite powders, nearly all of the surfaces of flaky Al powders were fully covered by CNTs (Fig. 5(c)).

The adsorption of high volume fraction of CNTs was related with large specific surface area of flaky Al powders. According to a simple geometric calculation, for the flaky Al powders with a thickness of about 500 nm, about 8 vol% CNTs could be adsorbed on flaky Al powders (CNT average diameter of 20 nm) when Al surfaces are fully covered by CNTs. It is important to point out that although the CNT adsorption was due to dipole/dipole electrostatic interaction of the zwitterionic surfactant, CNTs still remained on flaky Al powders when the zwitterionic surfactants were resolved after heat treatment.

It should be pointed out that although Kondoh et al. [24–26] also used zwitterionic surfactant for fabricating the CNT/Al composites, however, surfactant was only used as dispersant and no flaky Al powders were used. In this case, CNTs were not singly dispersed in the fabricated composites and the CNT concentration was low (~1 vol%).

3.3. Characterization of the CNT/Al composites

Fig. 6 shows the CNT distribution in forged 1.5 and 3 vol% CNT/Al composites. Three phenomenons could be observed. Firstly, CNTs were uniformly dispersed in the Al matrix, which was in accordance with the results of composite powders shown in Fig. 5. The CNT distribution uniformity was as good as that in the composites fabricated by Jiang et al. [31], and much better than that in the composites fabricated by other solution assisted wet mixing processes [23,24,32]. Furthermore, the matrix grains were of elongated shapes and most of CNTs tended to be distributed at the elongated-grain boundaries. Secondly, the dispersed CNTs were straight and aligned paralleled to the radius direction of the forged disk-shape samples. As described in Fig. 5, CNTs were located on the surface of flaky Al powders. Flaky Al powders tended to pack layer by layer during consolidation, and then CNTs tended to be distributed perpendicular to the hot-pressing direction after hot-pressing. During the forging process, CNTs could move with the plastic deformation of the Al matrix and were straightened due to the strain. As a result, aligned and straightened CNTs were observed. Thirdly, relatively long CNTs were observed. As shown in Fig. 6, 0.5–1 μm long CNTs (average length of about 0.9 μm, counting about 50 CNTs) was retained after forging. This length was similar with that of CNTs in the solution (Fig. 2(c)) and much longer than that observed in the CNT/Al composites fabricated by mechanical milling processes [13], which means low damage of the CNT macro-structure during fabrication.

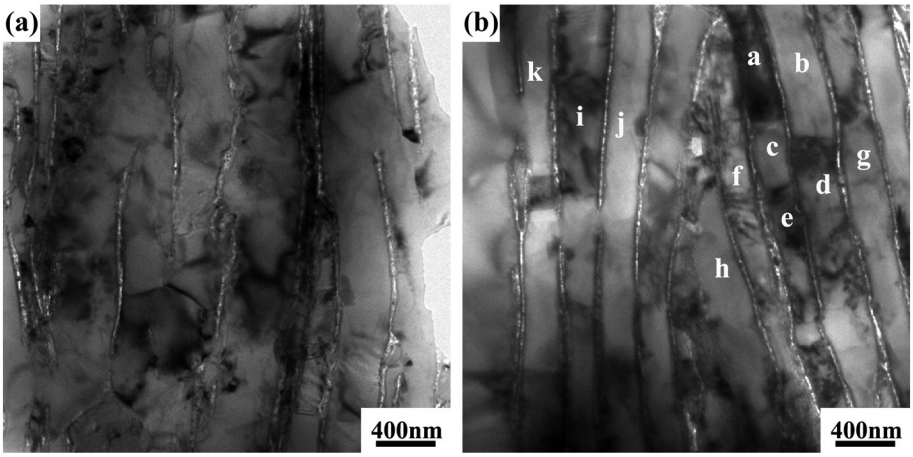

Fig. 6. TEM images showing CNT distribution in as-forged (a) 1.5 vol% and (b) 3 vol% CNT/Al composites. Zones marked with "a-k" had different contrasts, representing different grains.

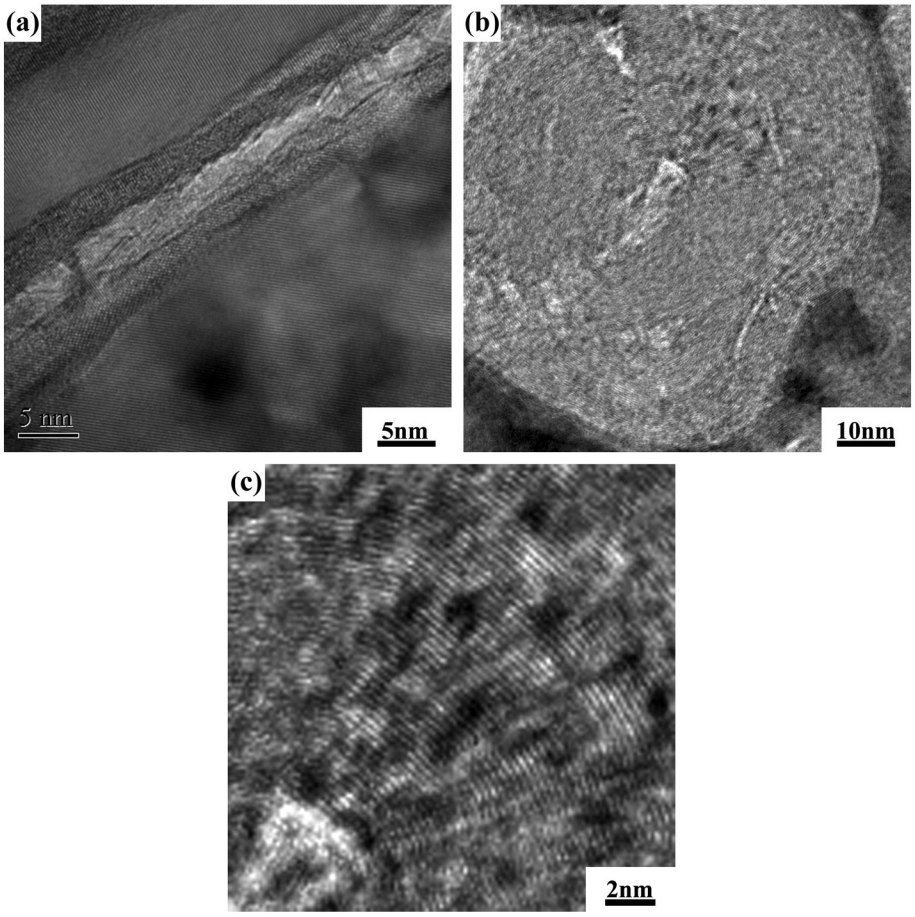

Fig. 7. HRTEM images showing (a) CNT-Al interface along CNT axis, (b) CNT-Al interface along cross-section of CNT and (c) CNT tube structure.

Fig. 7 shows the HRTEM images of the forged CNT/Al composites. Typical CNTs were shown in Fig. 7(a), which indicated that inner-outer tube of the CNTs was still retained, which also reflects little damage of the CNT macro-structure. The grains at different sides of CNTs were of different orientations, which indicated that CNTs were distributed at grain boundaries, and this is in agreement with the results shown in Fig. 6. No interface reaction products were observed at the CNT-Al interface (Fig. 7(a) and (b)), which was attributed to lower fabrication temperature and slight damage of CNTs. Furthermore, no obvious defect or void could be observed at the CNT-Al interfaces (Fig. 7 (a) and (b)), which indicates good bonding between CNT and Al. Although the shape of the CNT intersection surface was not perfect circle (shown in Fig. 7(b), related with the chemical vapor deposition and functionalization processes), the HRTEM image shown in Fig. 7 (c) indicated that the CNT tube structure was still retained, and interlayer spacing was about 0.34 nm, which was similar to that of the graphite.

The tensile strengths of the CNT/Al composites were significantly increased compared with those of the Al matrix. As shown in Fig. 8(a), 1.5 vol% CNT/Al composites showed a tensile strength of 334 MPa, while 3 vol% CNT/Al composite exhibited a tensile strength of 421 MPa, which is about 70% larger than that of the unreinforced Al matrix. Moreover, the ultimate tensile strength (UTS) of the CNT/Al composites increased linearly as the CNT concentration increased (shown in Fig. 8(b)), which confirmed the reinforcing effect of the CNTs.

For the CNTs reinforced metal matrix composites, an applied force can be transferred from the matrix to CNTs by a shear stress that is developed along the CNT-Al interface. Thus, it generates a variation in stress along the CNT length; the stress on CNTs increases proportionally from the CNT end to reach a critical value at the mid-region when the

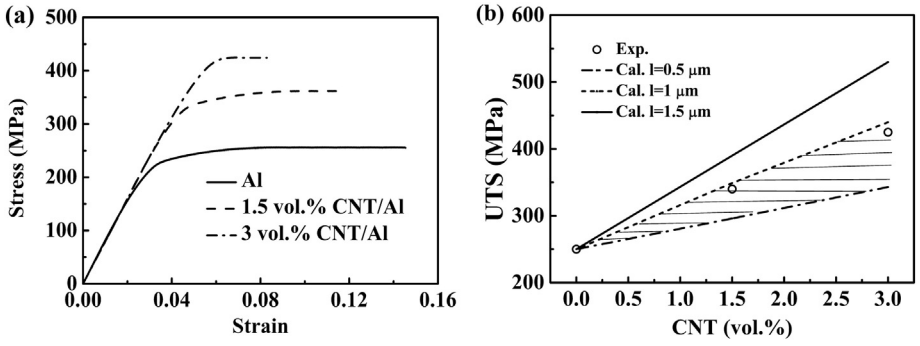

Fig. 8. (a) Engineering stress-strain curves, (b) comparison between theoretically predicted and experimentally measured UTS for CNT/Al composites.

Table 2
Comparisons of CNT/Al composites fabricated by various processes.

Ref.	Dispersing method	CNT distribution	CNT morphology	CNT damage	Tensile properties	Fabrication efficiency
[34]	Long time milling	Uniform	Length > 300 nm Diameter ~ 20 nm	Severe	0 vol% YS 255 MPa El 12% 3 vol% YS 450 MPa El 2%	High
[35]	Short time milling	Small pitch of clusters	Length ~ 800 nm Diameter ~ 140 nm	Normal	3 vol% YS 350 MPa	High
[32]	Nature rubber assisted wet mixing	Clusters	Length ~ 500 nm Diameter ~ 10 nm	Little	0 vol% UTS 80 MPa El 14% 5 vol% UTS 200 MPa El 8%	Medium
[24]	Zwitterionic assisted wet mixing	Clusters	–	Little	0 vol% UTS 160 MPa El 20% 1.2 vol% UTS 170 MPa El 22%	Medium
[31]	Flaky powder metallurgy	Uniform	Length > 500 nm Diameter 30–50 nm	Little	0 vol% YS 250 MPa EL 16% 2 vol% YS 380 MPa El 4%	Low
This article	Solution assisted wet mixing	Uniform	Length ~ 900 nm Diameter 10–40 nm	Little	0 vol% YS 240 ± 6 MPa El 12 ± 2% 1.5 vol% YS 306 ± 13 MPa El 8 ± 1% 3 vol% YS 410 ± 15 MPa El 4 ± 0.5%	Medium

CNT length is larger than the critical length (l_c) defined as:

$$l_c = \frac{\sigma_{CNT}}{\sigma_m} d \tag{1}$$

where σ_m is the UTS of the matrix (~250 MPa), σ_{CNT} is the strength of the CNT (~30 GPa) and d is the average diameter of CNTs (about 20 nm). The calculated l_c for the CNT/Al composites is about 2.4 μm, which is larger than the CNT length (0.9 μm). This means that the stress on CNTs could impossibly reach the fracture strength of CNTs. Thus, the strength and modulus of the composites could not be calculated by the rule of mixture. The strength of the CNT/Al composites are greatly related to the CNT length (l) and can be estimated through shear lag model [33] given as:

$$\sigma_c = \sigma_m(1-V_{CNT}) + kV_{CNT}\sigma_{CNT}\left(\frac{l}{2l_c}\right) \tag{2}$$

where σ_c is the strength of the composite, V_{CNT} is the volume fraction of CNTs and k reflects the load-transfer efficiency and is equal to 1, assuming that the matrix can transfer the load entirely.

As seen in Fig. 8(b), the calculated strength using Eq. (2) reasonably agrees with the experimental data. The concentration-dependence of UTS corresponds to a CNT length of only a little shorter than 1 μm, which matches well with the TEM results shown in Fig. 6. This also means that the load transfer efficiency from the matrix to the CNTs is high, in spite of the relatively short CNTs (0.9 μm) being retained compared to the as-received ones (0.5–2 μm). The strengthening of the composites was mainly attributed to the homogeneous distribution of CNTs in the Al matrix, good CNT-Al interface bonding and low damage of the CNT structure. It also reflects the practicability and validity of the fabrication route based on solution assisted wet mixing process and powder metallurgy.

Table 2 compares various CNT/Al composites fabricated by different processes. Compared with milling process, this solution assisted wet mixing process reduced CNT clustering and structure damage, thus the corresponding composites exhibited a good combination of strength and ductility, although the fabrication efficiency was still lower than that of milling. The tensile properties of the CNT/Al composites fabricated by our method reached the same level as those reported by Jiang et al. [31]. It is important to point out that this processing route does not involve the processes of Al powder pre-treatment and repeated rinsing-filtering. Therefore, it has a much higher efficiency and lower risk of reaction between Al powders and water.

4. Conclusions

An efficient solution assisted wet mixing process was developed to disperse CNTs, in which CNTs were adsorbed on flaky Al powders by using zwitterionic surfactant aqueous solution. The maximum CNT concentration of the CNT/Al composite powders could reach 7.5 vol%. 1.5 and 3 vol% CNT/Al composites were fabricated by a powder metallurgy route, producing greatly increased tensile strength, which is attributed to uniform distribution and little structure damage of CNTs as well as well bonded CNT-Al interface. The experimentally determined strength was in good agreement with calculated one by shear lag model, which demonstrated the high efficiency of the load-transfer from the Al matrix to CNTs.

Acknowledgements

The authors gratefully acknowledge the support of (a) the National Basic Research Program of China under grant nos. 2011CB932603 and 2012CB619600, (b) the CAS/SAFEA International Partnership Program for Creative Research Teams and (c) the National Natural Science Foundation of China under grant no. 51501189.

References

[1] J.M. Torralba, C.E. da Costa, F. Velasco, P/M aluminum matrix composites: an overview, J. Mater Proce Technol. 133 (2003) 203.
[2] Z.Y. Liu, Q.Z. Wang, B.L. Xiao, Z.Y. Ma, Y. Liu, Experimental and modeling investigation on SiCp distribution in powder metallurgy processed SiCp/2024 Al composites, Mater. Sci. Eng. A 527 (2010) 5582–5591.
[3] D.B. Miracle, Metal matrix composites — from science to technological significance, Compos. Sci. Technol. 65 (2005) 2526–2540.
[4] S.C. Tjong, Recent progress in the development and properties of novel metal matrix nanocomposites reinforced with carbon nanotubes and graphene nanosheets, Mater. Sci. Eng. R 74 (2013) 281–350.
[5] H. Kwon, M. Takamichi, A. Kawasaki, M. Leparoux, Investigation of the interfacial phases formed between carbon nanotube and aluminum in bulk material, Mater. Chem. Phys. 138 (2013) 787–793.
[6] C. Subramaniam, Y. Yasuda, S. Takeya, S. Ata, A. Nishizawa, D. Futaba, et al., Carbon nanotube-copper exhibiting metal-like thermal conductivity and silicon-like thermal expansion for efficient cooling of electronics, Nanoscale 6 (2014) 2669–2674.
[7] S.J. Yoo, W.J. Kim, Strength enhancement by shear-flow assisted dispersion of carbon nanotubes in aluminum matrix composite, Mater. Sci. Eng. A 570 (2013) 102–105.
[8] J. Cho, A. Boccaccini, M. Shaffer, Ceramic matrix composites containing carbon nanotubes, J. Mater. Sci. 44 (2009) 1934–1951.
[9] R. Perez-bustamante, F. Perez-Bustamante, I. Estrada-Guel, L. Licea-Jimenez, M. Miki-Yoshida, R. Martinez-Sanchez, Effect of milling time and CNT concentration on hardness of CNT/Al2024 composites produced by mechanical alloy, Mater. Charact. 75 (2013) 13–19.
[10] H.J. Choi, J.H. Shin, D.H. Bae, The effect of milling conditions on microstructures and mechanical properties of Al/MWCNT composites, Composites A 43 (2012) 1061–1072.
[11] A.M.K. Esawi, K. Morsi, A. Sayed, M. Taher, S. Lanka, The influence of carbon nanotube (CNT) morphology and diameter on the processing and properties of CNT-reinforced aluminium composites, Composites A 42 (2011) 234–243.
[12] K. Morsi, A.M.K. Esawi, S. Lanka, A. Sayed, M. Taher, Spark plasma extrusion (SPE) of ball-milled aluminum and carbon nanotube reinforced aluminum composite powders, Composites A 41 (2010) 322–326.
[13] J. Stein, B. Lenczowski, E. Anglaret, N. Frety, Influence of the concentration and nature of carbon nanotubes on the mechanical properties of AA5083 aluminium alloy matrix composites, Carbon 77 (2014) 44–52.
[14] T. Peng, I. Chang, Mechanical alloying of multi-walled carbon nanotubes reinforced aluminum composite powder, Powder Technol. 266 (2014) 7–15.

[15] Z.Y. Liu, B.L. Xiao, W.G. Wang, Z.Y. Ma, Developing high-performance aluminum matrix composites with directionally aligned carbon nanotubes by combining friction stir processing and subsequent rolling, Carbon 62 (2013) 35–42.
[16] Z.Y. Liu, B.L. Xiao, W.G. Wang, Z.Y. Ma, Analysis of carbon nanotube shortening and composite strengthening in carbon nanotube/aluminum composites fabricated by multi-pass friction stir processing, Carbon 69 (2014) 264–274.
[17] K.T. Kim, J. Eckert, S.B. Menzel, T. Gemming, S.H. Hong, Grain refinement assisted strengthening of carbon nanotube reinforced copper matrix nanocomposites, Appl. Phys. Lett. 92 (2008) 121901–121903.
[18] Y.J. Jeong, S.I. Cha, K.T. Kim, K.H. Lee, C.B. Mo, S.H. Hong, Small 3 (2007) 840–844.
[19] L. Cao, Z. Li, G. Fan, L. Jiang, D. Zhang, W.J. Moon, et al., The growth of carbon nanotubes in aluminum powders by the catalytic pyrolysis of polyethylene glycol, Carbon 50 (2012) 1057–1062.
[20] X. Yang, E. Liu, C. Shi, C. He, J. Li, N. Zhao, K. Kondoh, Fabrication of carbon nanotube reinforced Al composites with well-balanced strength and ductility, J. Alloy Comp. 563 (2013) 216–220.
[21] S. Cho, K. Kikuchi, T. Miyazaki, A. Kawasaki, Y. Arami, J.F. Silvain, Epitaxial growth of chromium carbide nanostructures on multiwalled carbon nanotubes (MWCNTs) in MWCNT–copper composites, Acta Mater. 61 (2013) 708–716.
[22] C. Deng, X. Zhang, D. Wang, Q. Lin, A. Li, Preparation and characterization of carbon nanotubes/aluminum matrix composites, Mater. Lett. 61 (2007) 1725–1728.
[23] J.F. Liao, M.J. Tan, I. Sridhar, Spark plasma sintered multi-wall carbon nanotube reinforced aluminum matrix composites, Mater. Des. 31 (2010) S96–S100.
[24] K. Kondoh, H. Fukuda, J. Umeda, H. Imai, B. Fugetsu, Microstructural and mechanical behavior of multi-walled carbon nanotubes reinforced Al–Mg–Si alloy composites in aging treatment, Carbon 72 (2014) 15–21.
[25] K. Kondoh, H. Fukuda, J. Umeda, H. Imai, B. Fugetsu, M. Endo, Microstructural and mechanical analysis of carbon nanotube reinforced magnesium alloy powder composites, Mater. Sci. Eng. A 527 (2010) 4103–4108.
[26] K. Kondoh, T. Threrujirapapong, H. Imai, J. Umeda, B. Fugetsu, Characteristics of powder metallurgy pure titanium matrix composite reinforced with multi-wall carbon nanotubes, Compos. Sci. Technol. 69 (2009) 1077–1081.
[27] L. Jiang, G. Fan, Z. Li, X. Kai, D. Zhang, Z. Chen, et al., An approach to the uniform dispersion of a high volume fraction of carbon nanotubes in aluminum powder, Carbon 49 (2011) 1965–1971.
[28] B. Fugetsu, W. Han, N. Endo, Y. Kamiya, T. Okuhara, Disassembling single-walled carbon nanotube bundles by dipole/dipole electrostatic interactions, Chem. Lett. 34 (2005) 1218–1219.
[29] W. Huang, Y. Lin, S. Taylor, J. Gaillard, A. Rao, Y. Sun, Sonication-assisted functionalization and solubilization of carbon nanotubes, Nano Lett. 2 (2002) 231–234.
[30] O. Matarredona, H. Rhoads, Z. Li, J. Harwell, L. Balzano, D. Resasco, Dispersion of single-walled carbon nanotubes in aqueous solutions of the anionic surfactant NaDDBS, J. Phys. Chem. B. 107 (2003) 13357–13367.
[31] L. Jiang, Z. Li, G. Fan, L. Cao, D. Zhang, The use of flake powder metallurgy to produce carbon nanotube (CNT)/aluminum composites with a homogenous CNT distribution, Carbon 50 (2012) 1993–1998.
[32] H. Kwon, M. Estili, K. Takagi, T. Miyazaki, A. Kawasaki, Combination of hot extrusion and spark plasma sintering for producing carbon nanotube reinforced aluminum matrix composites, Carbon 47 (2009) 570–577.
[33] Y. Wu, E.J. Lavernia, Metall. Mater. 27 (1992) 173–178.
[34] H.J. Choi, J.H. Shin, B.H. Min, J.S. Park, D.H. Bae, Reinforcing effects of carbon nanotubes in structural aluminum matrix nanocomposites, J. Mater. Res. 24 (2009) 2610–2616.
[35] A.M.K. Esawi, K. Morsi, A. Sayed, M. Taher, S. Lanka, Effect of carbon nanotube (CNT) content on the mechanical properties of CNT-reinforced aluminium composites, Compos. Sci. Technol. 70 (2010) 2237–2241.